J. Plasma Fusion Res. SERIES, Vol. 4 (2001) 43–47

Internal Transport Barriers in W7-AS

STROTH Ulrich[1*], ITOH Kimitaka[2], ITOH Sanae-I.[3], HARTFUß Hans, LAQUA Heinrich, the ECRH and the W7-AS Team
MPI für Plasmaphysik, EURATOM Association, D-85748 Garching, Germany
[1]Institut für Experimentelle und AngewandtePhysik, CAU Kiel, Germany
[2]National Institute for Fusion Science, Toki, Gifu 509-5292, Japan
[3]Kyushu University, Kasuga 816-8580, Japan

(Received: 5 December 2000 / Accepted: 16 August 2001)

Abstract

The three-dimensional magnetic configuration of a stellarator offers a specific mechanism for a transition to improved particle and energy confinement. The pathway opens due to the layer of a strongly varying radial electric field which is present in the transitional region from neoclassical electron to ion-root confinement. This type of improvement acts on turbulent transport.

Keywords:

W7-AS, internals transport barrier, neoclassical transport

1. Introduction

Transport of energy and particles in magnetically confined high-temperature plasmas is in general strongly enhanced above the neoclassical transport, i.e. the collisional flux-level estimates. The enhancement is attributed to turbulence and this is independent of the specific magnetic configuration. Systems with toroidal symmetry, like tokamaks, show the same level of transport as devices without this symmetry, like helical systems [1,2]. For the construction of a fusion power reactor, a transport reduction with respect to the so-called L-mode confinement level is needed. The most efficient reductions achieved are by transport barriers, where in a radially limited area the diffusion coefficients are reduced to the collisional level. The most prominent transport barriers known are the H-mode [3] and the so-called internal transport barriers (ITB) [4]. It is generally accepted that the turbulence reduction is due to a sheared poloidal plasma flow generated by a radially varying radial electric field (See for a review, e.g., [5,6]).

The three-dimensional magnetic field configuration of stellarators bears an additional loss channel for particles and energy. It opens due to the collisionless loss of particles trapped in local magnetic mirrors. The related particle fluxes are non-ambipolar and hence they create a radial electric current to modify the radial electric field. This electric field generation opens two stellarator-specific routes to transport reduction: The neoclassical electron root (ER) and in addition the formation of a neoclassically driven internal transport barrier in the transition layer from electron-root to ion-root (IR) confinement.

Generally, in both cases a plasma with strongly heated electrons is needed to make electron losses superior to ion losses. In the plasma center, the plasma potential turns from negative or small positive to strongly positive values. This feature is called the electron root and has been observed in CHS [7,8] and in W7-AS [9,10] right in the plasma core. The electron root is characterized by a strong reduction of the

**Corresponding author's e-mail: stroth@physik.uni-kiel.de*

neoclassical transport within the region where a strong positive electric field exists. The neoclassical diffusivity drops to values of the order of 0.1 m^2/s. An additional potential for transport reduction occurs at the transition layer from the electron root to the ion root regime. In this region the potential changes from strongly positive to small or negative values. It therefore consists of a layer with strongly sheared plasma flow, which is able to reduce turbulent transport.

This article discusses the observations in relation with a transport barrier in the transition layer between the two neoclassical regimes [11] and focusses on the hysteresis in the transition with respect to a neoclassical transition.

The neoclassical process leading to the transition is discussed in Fig. 1. For three values of the electron temperature, it shows neoclassical electron and ion fluxes as function of the radial electric field. The ion

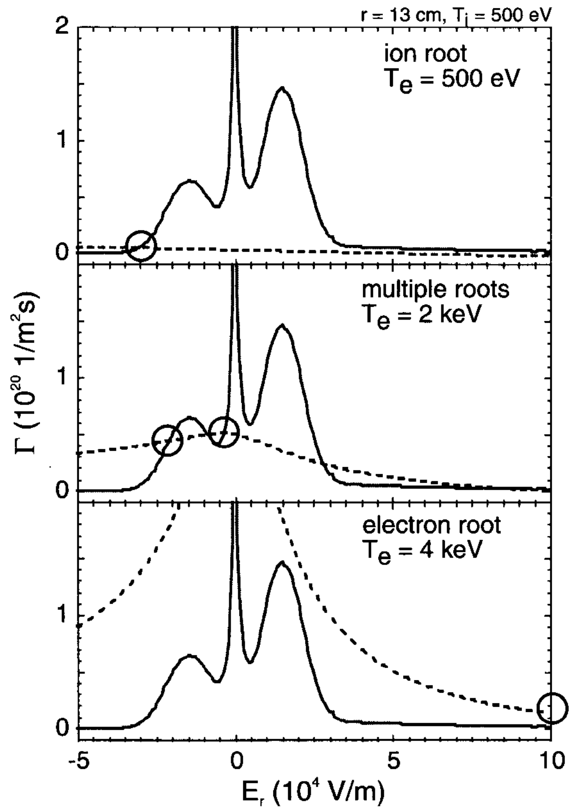

Fig. 1 Neoclassical electron (dashed) and ion (full line) transport as function of the radial electric field for T_i = 500 eV and three value of T_e. The calculation is done with the DKES code for W7-AS at a radius of 13 cm. Circles indicate where the ambipolarity condition is sattisfied.

temperature is fixed at 500 eV. The central peak is caused by the loss of hellically trapped particles while the two other bumps are due to the toroidal resonance. Due to the higher velocity, in the electron transport only the hellically trapped particles can be seen as T_e increases. Ambipolarity is satisfied where the two lines intersect. At T_e = 500 eV, only one solution is found corresponding to the ion-root. At the intermediate T_e value, three solution are possible. A small change in T_e can lead to strong changes in E_r. At the highest T_e, which corresponds to a situtation, where experimentally an electron-root was found, only one solution is obtained at strongly positve E_r. In the figure it can be seen that, once the electron-root is realized, T_e has to drop to very small values until a back transition to the ion-root occurs. Hence, a neoclassical transition will have a very strong hysteresis in T_e.

In the following a regime will be investigated where a shear layer co-exists with the ER regime, where the neoclassical transport must be very low. Therefore, a turbulence suppression in the radially limited shear layer will lead to a transport barrier with a strong increase of the temperature gradient. The structure of transport barriers has been discussed in [12-14]. Since the development of a transport barrier depends in a non-local way on plasma parameters, a hysteresis both in electron temperature T_e and heating power P should appear [15].

2. Experimental Results

Figure 2 depicts contours of the ECE electron temperature from a W7-AS discharge undergoing several pronounced forth and back transitions into improved core confinement. The core temperature increases by 0.7 keV to about 4.8 keV. The line average density was $\bar{n}_e = 3.5 \times 10^{19}$ m^{-3}, the magnetic field strength B = 2.5 T, the rotational transform ι = 0.34 and the heating power P = 1.27 MW. The presented phase of the discharge has parameters sufficient to access the neoclassical electron-root regime; details of the discharge can be found in [10,11]. Fig. 2 depicts the increment of the electron temperature at various radii. Negative radii indicate the high-field side of the plasma. It can be seen, that the modification of the electron temperature due to the transitions is concentrated to the plasma core with an effective radius of $|r| \leq 6$ cm. The asymmetry between high and low-field side is due to imperfect correction of the Shafranov shift. Hence one has to symmetrizes the data. The increase of the electron temperature is almost the same in the inner region. This indicates that the improvement is due to a localized transport barrier.

In Fig. 3, the change of the temperature gradient is explored. The data were obtained by taking the differences of adjacent channels and dividing them by the radial separation. Due to the Shafranov shift, one has to symmetrize to obtain the radial information. Since radiative losses and ion-electron coupling are negligible in the core, the time traces are closely related to the thermal diffusivity. The increment of $\mathrm{d}T_e/\mathrm{d}r$ amounts up to 0.4 keV/cm, which is approximately twice the gradient in the low confinement regime. Absolute values for the electron heat diffusivity deduced from adjacent ECE channels at $r \approx 4$ cm during the improved phase are in the range of 0.2 m^2/s and the reduction is of the order of 50 %. It is found that the increment of the temperature gradient is localized near the surface around $r \approx 4$ cm. The full width of the layer in which $\mathrm{d}T_e/\mathrm{d}r$ increases is about 3 cm. This implies that the reduction in transport, which drives the incremental jump of the central electron temperature, is restricted to a narrow layer around $r \approx 4$ cm. For the inner channels, rather a decrease of the gradient than an increase is observed.

Theoretical neoclassical estimates using the DKES code [16,17] yield that the discharge should transit into the electron-root regime already at an electron temperature of 2 keV. Hence the depicted phase with $T_e(0) \approx 4.5$ eV should be deeply in the ER state and transitions seen at 4 keV are not consistent with a neoclassical prediction for the access of the ER state. The radial region of ER confinement is predicted to be inside 6 cm. This would lead to a shear layer at about 6 cm and would be consistent with the interpretation, that confinement improvement is due to a transport barrier in the neoclassically generated shear layer. Furthermore, the observation of a diffusivity well below 1 m^2/s shows that turbulent transport is strongly suppressed. As a third point in favour of a transport barrier, the hysteresis behavior of the transition is discussed below.

A consistent picture emerges as follows: The phase of the discharge shown in Figs. 2 and 3 is in the ER state throughout. Therefore, already prior to the transitions the shear layer can have already a reducing impact on turbulence. This explains the low value of $\chi_e \approx 0.5$ m^2/s in the low confinement phase. The jump in electron temperature can then be attributed to the development of a transport barrier, where the sheared flow fully stabilizes the turbulence. The responsible radial electric field is mainly provided by the neoclassical particle flux but also influences by the

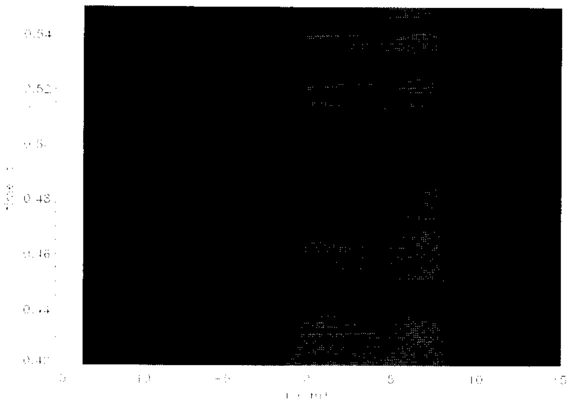

Fig. 2 ECE measurements of the electron temperature in discharge 42975 with multiple transitions low and improved confinement. The average tempearture was substracted from each ECE channel, hence the data represent the increment during the transitions.

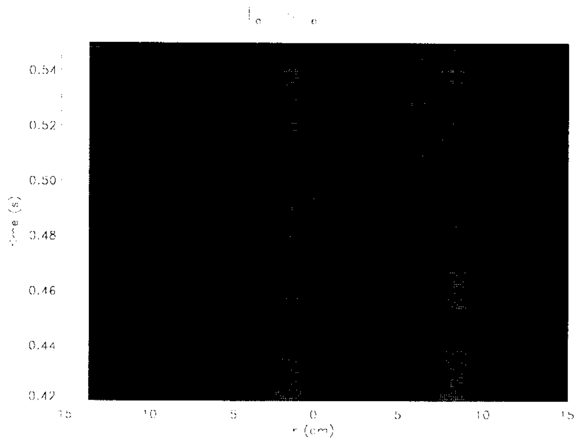

Fig. 3 Change of Electron temperature gradient estimated from the data of discharge 42975 shown in Fig. 2.

vertical drift of non-thermal electrons generated by the intense ECRH.

3. Evidence for Bifurcations

The bifurcation behavior of the transport barrier was investigated by power-ramp experiments. The plasma parameters were $B = 2.5$ T, $\bar{n}_e = 1 \times 10^{19}$ m^{-3} and $\iota \approx 1/3$. The power was ramped down from 0.7 MW to 0.3 MW and ramped back up again (see upper trace in Fig. 4). Fig. 4 shows the resulting time traces of the electron temperature at three inner radii. The discharge

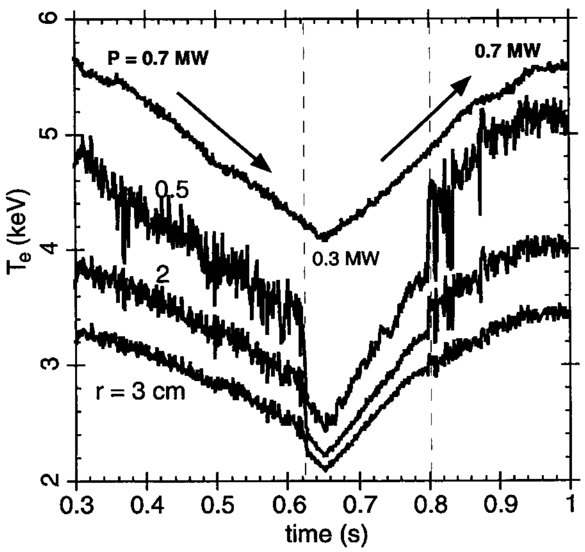

Fig. 4 Heating power (top curve) and three channels (radii in centimeters are indicated) of the ECE electron temperature diagnostics in the power-ramp discharge 46388.

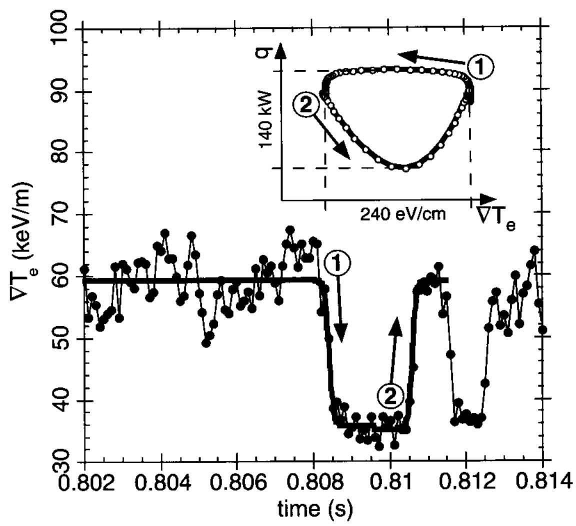

Fig. 5 The temperature gradient of the dithering phase shown in Fig. 4 calculated from the time traces for $r = 0.5$ and 3 cm. For one cycle a fit is also shown (solid line). From the fit, the insert is calculated, which shows the hysteresis of power flux vs. temperature gradient during the cycle. The distance in the time steps of the insert is 0.02 ms.

in the time frame of Fig. 4 starts in the improved regime. In these discharges, an effect of transport reduction is only observed at $r \leq 3$ cm. This might be due to the reduced available power of 0.7 MW.

At 0.62 s the back transition into the low confinement occurs at a heating power of 0.34 MW. The temperatures at the three radii are 3.4, 2.8 and 2.4 keV, respectively. Due to the back transition, the temperature difference between $r = 2$ cm and $r = 3$ cm drops by more than 60 %, and that between $r = 0.5$ cm and $r = 2$ cm by more than 50 %. This reduction in the gradient reflects the strong increase of total transport at the back transition. After increasing the power again, the transition into improved confinement is observed at a heating power of 0.5 MW and temperatures of 3.8, 3.2 and 3.0 keV. Hence the data show a hysteresis in both temperature and heating power. After the transition into the improved state, the temperature difference between $r = 2$ cm and $r = 3$ cm increases by a factor of two and is the same as between $r = 0.5$ cm and $r = 2$ cm. This indicates the reduction of the energy transport coefficient by about a factor of two. These prominent jumps of the transport coefficient (which is dominated by anomalous transport) at both transitions clearly illustrates the existence of the transport barrier for the electron energy. Neoclassical calculations of the hysteresis are shown in Fig. 6. According to this figure, the back transition to the IR regime is expected at $T_e <$ 200 eV. This indicates that the sudden confinement improvement is due to a suppression of turbulent transport in a region which might be preconditioned by

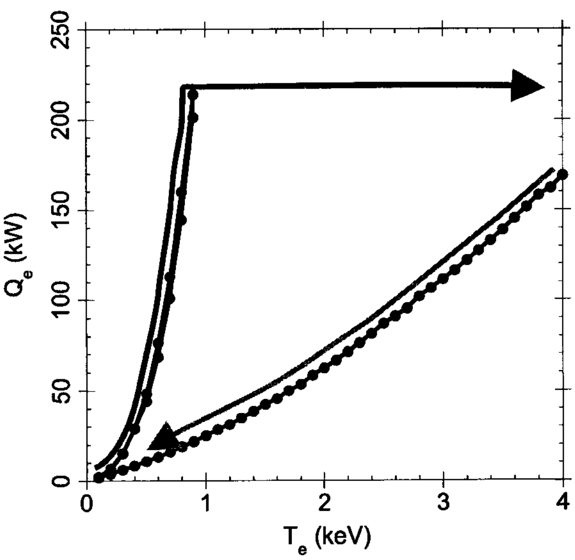

Fig. 6 Hysteresis expected according to the DKES code for the transitions from electron to ion-root regimes calcualted with the parameters of the discharge of Fig. 4.

neoclassical transport.

In the transition to the improved state (t = 0.8–0.84 sec), i.e. near the threshold condition, dithering cycles are observed. In Fig. 5, one of these cycles is analyzed in view of the hysteresis. To this end, the temperature data at r = 0.5 and 3 cm from Fig. 4 where used to calculate temperature gradient and average temperature. Both time traces were fitted to calculate the dependence of power flux (heating power corrected due to the temporal change of the energy content) on temperature gradient as plotted in the insert of Fig. 5. Data and fit of the temperature gradient are also depicted. The arrows indicate the course of time for the transition to low confinement (1) and back to improved confinement (2). The dots in the insert mark time points every 20 μs. The swing of the hysteresis in power flux is about 140 kW. This behavior shows again that it is not a smooth transition to improved confinement but rather the development of a barrier which can suddenly appears and vanish. The hysteresis occurs at very different values from those expected in a neoclassical transition as shown in Fig. 6.

4. Conculsions

In conclusion, several observations indicate that the confinement improvement observed in strongly ECR heated plasmas is due to the development of an internal transport barrier rather than due to a reduction of neoclassical transport in the electron root regime. The low value of the diffusivity points to a suppression of turbulent transport, the transport reduction appears in a narrow radial region and the forth and back transitions as well as the dithering phase prior to the transition exhibit a hysteresis in temperature and heating power at temperatures inconsistent with the neoclassical prediction for the ER transition. It can be conjectured that it is the flow shear layer inbetween the neoclassical electron- and ion-root regimes (possibly increased by drifts of non-thermal electrons produced by ECRH) which stabilizes turbulence and reduces the turbulent transport contribution in a narrow layer.

Acknowledgments

Two of the authors (KI and SII) acknowledges hospitality of Alexander von Humboldt Stiftung and Max-Planck-Institut fur Plasmaphysik.

References

[1] F. Wagner and U. Stroth, Plasma Phys. Control. Fusion **35**, 1321 (1993).

[2] U. Stroth, Plasma Phys. Control. Fusion **40**, 9 (1998).

[3] F. Wagner *et al.*, Phys. Rev. Lett. **49**, 1408 (1982).

[4] E.J. Strait *et al.*, Phys. Rev. Lett. **75**, 4421 (1995).

[5] K. Itoh and S.-I. Itoh, Plasma Phys. Controll. Fusion **38**, 1 (1996).

[6] K.H. Burrell *et al.*, Phys. Plasmas **4**, 1499 (1997).

[7] H. Idei *et al.*, Phys. Rev. Lett. **71**, 22 (1993).

[8] A. Fujisawa *et al.*, Phys. Rev. Lett. **86**, 2669 (1998).

[9] M. Kick *et al.*, Plasma Phys. Control. Fusion **41**, A549 (1999).

[10] H. Maassberg *et al.*, Phys. Plasmas **7**, 295 (2000).

[11] U. Stroth *et al.*, Phys. Rev. Lett. **86**, 5910 (2001).

[12] P.H. Diamond *et al.*, Phys. Plasmas **2**, 3685 (1995).

[13] P.H. Diamond *et al.*, Phys. Rev. Lett. **78**, 1472 (1997).

[14] K. Itoh, S.-I. Itoh and A. Fukuyama, *Transport and Structural Formation in Plasmas* (IOP, England, London, England, 1999), chapter 12.

[15] S.-I. Itoh and K. Itoh, Phys. Rev. Lett. **60**, 2276 (1988).

[16] W.I. van Rij and S.P. Hirshman, Phys. Fluids, B **1**, 563 (1989).

[17] H. Maaßberg *et al.*, Plasma Phys. Control. Fusion **35**, B319 (1993).